THE JOURNAL OF IMMUNOLOGY

Distinct Subsets of FoxP3+ Regulatory T Cells Participate in the Control of Immune Responses

Geoffrey L. Stephens, John Andersson and Ethan M. Shevach

J Immunol 2007; 178:6901-6911; ;
http://www.jimmunol.org/content/178/11/6901

The Journal of Immunology is published twice each month by
The American Association of Immunologists, Inc.,
9650 Rockville Pike, Bethesda, MD 20814-3994.

Print ISSN: 0022-1767 Online ISSN: 1550-6606.

Distinct Subsets of FoxP3$^+$ Regulatory T Cells Participate in the Control of Immune Responses[1]

Geoffrey L. Stephens, John Andersson, and Ethan M. Shevach[2]

Expression of the transcription factor FoxP3 is the hallmark of regulatory T cells that play a crucial role in dampening immune responses. A comparison of the development and phenotype of FoxP3$^+$ T cells in relation to the expression of conventional MHC molecules facilitated the identification of several distinct lineages of naive and effector/memory populations of Foxp3$^+$ T cells. One subpopulation of effector/memory Foxp3$^+$ T cells develops in the thymic medulla, whereas the second is thymic independent. Both lineages display a distinct activated phenotype, undergo extensive steady-state proliferation, home to sites of acute inflammation, and are unique in their capacity to mediate Ag-nonspecific suppression of T cell activation directly ex vivo. Effector FoxP3$^+$ T cells may act as a sentinel of tolerance, providing a first line of defense against potentially harmful responses by rapidly suppressing immunity to peripheral self-Ags. *The Journal of Immunology,* **2007, 178: 6901–6911.**

Regulatory T cells play a major role in the control of all immune responses. Although T cells with regulatory activity have been described as expressing multiple phenotypes (1), the most prominent population of T regulatory cells in mice and humans is the CD4$^+$CD25$^+$ subset that expresses the transcription factor Foxp3 (2–6). The regulatory mechanisms used by Foxp3$^+$ T cells in vitro and in vivo are heterogeneous and their suppressor effector functions can be mediated by both cell contact-dependent and cytokine-dependent pathways (7). Similarly, in mice, Foxp3$^+$ regulatory T cells display a mixed cell surface phenotype consisting of Ags associated with both activated and naive T cells (8, 9). Taken together, these findings have raised the possibility that some of the activities of the Foxp3$^+$ population are mediated by distinct subsets.

The one phenotypic marker that potentially distinguishes a unique functional subset of Foxp3$^+$ T cells is expression of the integrin $\alpha_E\beta_7$ (CD103). Although CD103 is expressed on CD4$^+$ and CD8$^+$ T cells in the intestine and other epithelial compartments, only 20–30% of CD4$^+$CD25$^+$ T cells express CD103 and expression is not up-regulated by T cell activation in vitro (10–12). A number of studies have suggested that the CD4$^+$CD25$^+$ CD103$^+$ subset may play a specialized functional role in T cell-mediated suppression. CD4$^+$CD25$^+$CD103$^+$ T cells were shown to display a cell surface Ag profile resembling effector/memory T cells, to be more potent suppressors of the activation of CD4$^+$ CD25$^-$ T cells in vitro, and to selectively home to inflamed tissue sites in vivo (10, 11, 13).

A second approach to the analysis of the functional heterogeneity of CD4$^+$CD25$^+$ T regulatory cells has been to examine their behavior in vivo in normal unmanipulated mice. Fisson et al. (14) identified two distinct subsets of CD4$^+$CD25$^+$ T cells. One subpopulation was quiescent and appeared to have a long lifespan, while the second subpopulation divided extensively, expressed multiple activation markers, and expanded preferentially in lymph nodes (LNs)[3] expressing target autoantigens. One caveat in the interpretation of these studies was that expression of Foxp3 was not studied and it remained possible that some of the rapidly dividing cells were derived from a small number of CD4$^+$CD25$^+$ effector cells that contaminated the T regulatory cells.

Several lines of evidence indicate that most Foxp3$^+$ regulatory T cells develop in the thymus. Some reports have suggested that differentiation of immature thymocytes toward the FoxP3 lineage is the result of high-affinity TCR/MHC class II interactions (15), although more recent work suggests an alternative interpretation (16). It has been widely accepted that TCR/MHC class II Ags provide instructive signals for the development of CD4$^+$FoxP3$^+$ T cells. Expression of MHC class II molecules on cortical thymic epithelium was both necessary and sufficient for inducing CD4$^+$ FoxP3$^+$ regulatory T cell development (17). This conclusion was supported by the observation that a peripheral CD4$^+$CD25$^+$ subset present in MHC class II-deficient (MHC II$^{-/-}$) animals, which phenotypically resembled regulatory T cells, lacked functional suppressor activity (17).

The availability of both Abs to Foxp3 as well as mice expressing fluorochromes under the control of the Foxp3 promoter has also suggested that heterogeneity may exist among Foxp3$^+$ T regulatory cells (18, 19). Although the majority of FoxP3$^+$ cells in wild-type mice appear to require MHC class II expression for their thymic development, subsets of FoxP3$^+$CD8$^+$ T cells are present in the thymus of both wild-type and MHC class II-deficient (MHC II$^{-/-}$) mice (19). Furthermore, the periphery of MHC II$^{-/-}$ mice contains CD8$^+$CD25$^+$ T cells that exhibit contact-dependent suppressive activity analogous to that mediated by wild-type CD4$^+$CD25$^+$ T cells (20). Other reports have indicated that a unique subset of CD4$^+$CD8$^+$CD25$^+$ T cells in MHC II$^{-/-}$ mice is enriched in FoxP3 mRNA and capable of suppressing T cell-mediated inflammatory bowel disease (21). Curiously, while prevalent in MHC II$^{-/-}$ mice, CD8$^+$CD25$^+$ T cells are quite rare in wild-type animals (20).

Cellular Immunology Section, Laboratory of Immunology, National Institute of Allergy and Infectious Diseases, National Institutes of Health, Bethesda, MD 20892

Received for publication January 24, 2007. Accepted for publication March 22, 2007.

The costs of publication of this article were defrayed in part by the payment of page charges. This article must therefore be hereby marked *advertisement* in accordance with 18 U.S.C. Section 1734 solely to indicate this fact.

[1] This work was supported by the Intramural Research Program of the National Institutes of Health, National Institute of Allergy and Infectious Diseases.

[2] Address correspondence and reprint requests to Dr. Ethan M. Shevach, National Institutes of Health, Building 10, Room 11N315, 10 Center Drive, MSC-1892, Bethesda, MD 20892-1892. E-mail address: eshevach@niaid.nih.gov

[3] Abbreviations used in this paper: LN, lymph node; 7-AAD, 7-aminoactinomycin D; HA, hemagglutinin; β_2m, β_2-microglobulin; KLRG1, killer cell lectin-like receptor G1.

In this study, we present a comprehensive investigation of the development and phenotype of FoxP3$^+$ T cells in relation to the expression of conventional MHC molecules. To clarify the MHC requirements for the development of FoxP3$^+$ lineage T cells, we initially characterized mice lacking expression of various MHC-encoded molecules. Surprisingly, peripheral FoxP3$^+$ T cells are present in substantial numbers in mice lacking conventional MHC class II molecules or expression of the CD4 coreceptor. A small subset of Foxp3$^+$ T cells could be identified, in the periphery, but not in the thymus, in mice lacking all conventional MHC molecules. This subset also appears to be present in wild-type mice at levels comparable to those observed in the MHC class I/II-deficient strain. Both the thymus-dependent and the thymus-independent subsets displayed an effector/memory phenotype and exhibited considerable steady-state proliferation in vivo relative to the majority population found in wild-type mice. The thymus-dependent effector subset acquires an activated phenotype during development, which requires MHC expression in the medullary thymus. Consistent with their surface phenotype, the effector FoxP3$^+$ T cells from all of the strains examined demonstrated a unique capacity to mediate Ag-nonspecific suppression of T cell activation directly ex vivo without exogenous TCR triggering. Following an inflammatory stimulus, both subsets appear rapidly in the LNs draining the inflamed site. We speculate that distinct lineages of FoxP3$^+$ T cells may act as sentinels of tolerance, providing a first line of defense against potentially harmful responses by rapidly suppressing in an Ag nonspecific manner immunity to peripheral self-Ags.

Materials and Methods

Abs and reagents

The following Abs used for flow cytometric analysis were obtained from eBioscience: anti-FoxP3-PE, -allophycocyanin, -PE-CY5 (FKJ-16S), anti-CD103-FITC, -biotin (2E7), anti-CD25 -PE, -PE-TR, -PE-CY7, -PE-CY5 (PC61), anti-killer cell lectin-like receptor G1 (KLRG1)-biotin (2F1), anti-βTCR-allophycocyanin-CY7 (H57–597), anti-CD44-PE-CY5 (IM7), and anti-CD45.2-allophycocyanin (clone 104). The following Abs for flow cytometric analysis were obtained from Invitrogen Life Technologies-Caltag Laboratories: CD8-allophycocyanin-CY5.5 (5H10), anti-CD25-PE-CY5.5 (PC61), and anti-CD62L-PE-TR (MEL-14). The following Ab reagents for flow cytometric analysis and functional studies were obtained from BD Biosciences: anti-CD4-allophycocyanin, -PE-Cy5, -Pacific Blue (RM4-5), anti-CD8$^-$PE-CY7 (53-6.7), anti-CD24-FITC, biotin (M1/69), anti-CD45.1-PE (A20), anti-CD49b-(PE, allophycocyanin), anti-NK1.1-PE (PK136), anti-BrdU-FITC,-PE (3D4), purified anti-IL-10, purified anti-CD3 (3C11), Annexin V^{FITC}, streptavidin-allophycocyanin-CY7, -allophycocyanin-CY5.5, -allophycocyanin, and 7-aminoactinomycin D (7-AAD). Anti-TGF-β was obtained from R&D Systems. MHC class II-specific Abs (clone Y3P) were from purified ascites fluid. BrdU and LPS were obtained from Sigma-Aldrich.

Animals

C57BL/6 and BALB/c mice were obtained from the Department of Cancer Therapeutics (National Cancer Institute, Frederick, MD). Mice expressing a transgenic TCR specific for influenza hemagglutinin (HA) peptide, HA (110–119), were provided by Dr. H. von Boehmer (Dana-Farber Cancer Institute, Boston, MA) and maintained at Taconic Farms under National Institute of Allergy and Infectious Diseases contract. Mice deficient for K^{b}D^b, β_2-microglobulin (β_2m), A$^b\beta$, or doubly deficient for A$^b\beta$ and β_2m, K14, and CD45.1 congenic mice were all on the C57BL/6 background and obtained from Taconic Farms. Mice lacking all conventional MHC class II chains (22) (MHC II$^{\Delta/\Delta}$) and Thy1.1 congenic mice on the C57BL/6 background were obtained from The Jackson Laboratory. All mice were housed under specific pathogen-free conditions in accordance with institutional guidelines.

Flow cytometry

Thymus or LNs (axillary, inguinal, superficial cervical, mandibular, and mesenteric LNs) were harvested and single-cell suspensions were obtained by gentle passage through 40-μm nylon mesh filters (BD Biosciences). Following lysis of RBC using ACK lysis buffer and counting of viable cells, suspensions were preblocked using purified anti-CD16/32 Ab (2.4.G2) for 10 min. For thymocyte staining, the ACK lysis step was omitted from the procedure. Without further washing, surface staining was performed and samples were either subsequently analyzed or further processed as necessary.

Cell sorting and autoMACS purification

All T cell subsets were purified from peripheral LNs of mice. RBC were lysed with ACK lysis buffer (Biofluids). For purification of CD4$^+$CD25$^-$ cells, HA-specific TCR were stained with anti-CD25 PE and subsequently labeled with anti-PE magnetic microbeads and purified on an autoMACS (Miltenyi Biotec) according to the manufacturer's protocol. Cells remaining in the negative fraction were subsequently labeled with anti-CD4 microbeads and purified using the positive selection program on the autoMACS. Purity of the resulting samples was routinely 95–97%. CD4$^+$CD25$^+$ subsets were sorted by flow cytometry as previously described (8).

In vitro proliferation assays

Suppression assays were performed, as described (8). Briefly, (5×10^4) HA-specific CD4$^+$CD25$^-$ T cells were cocultured in DMEM supplemented with 7% heat-inactivated FCS, penicillin (100 U/ml), streptomycin (100 μg/ml), 2 mM L-glutamine, 10 mM HEPES, 0.1 mM nonessential amino acids, 1 mM sodium pyruvate (all from Biofluids), and 50 μM 2-ME, with irradiated (3000 R) T cell-depleted splenocytes (5×10^4) in the presence of either 0.5 μg/ml anti-CD3 mAb (2C11) or 16 μM HA (110–119)-peptide in 96-well flat-bottom plates. Titrated numbers of CD103$^+$ or CD103$^-$CD4$^+$CD25$^+$ T cells were added at final suppressor to responder ratios of 0:1 or 1:2. Cultures were pulsed with 1 μCi [^{3}H]thymidine for the final 8–10 h of a 72-h culture and were performed in triplicate unless otherwise indicated.

In vivo treatments

For experiments involving Ab treatments, mice were injected i.p. (2 mg/mouse) every other day over the course of 4 days with isotype control Abs or blocking Abs specific for MHC class II molecules (clone Y3P). On the fourth day, mice were injected i.v. with 1 mg of BrdU and subsequently analyzed. Alternatively, CD4$^+$CD25$^+$ subsets from harvested from LNs from treated animals were purified by FACS and used in suppression assays. For transfer experiments, CD4$^+$CD25$^+$ subsets were purified by FACS and labeled with CFSE as previously described (23) and transferred i.v. (5×10^5 cells/animal) into wild-type congenic CD45.1-expressing hosts. In other experiments, C57BL/6 mice were injected s.c. with 100 μg of LPS and after 5 days draining and nondraining LNs were harvested and stained for expression of surface markers and intracellular FoxP3.

Intracellular staining for BrdU and FoxP3

Cells were surface stained as described, washed, and then fixed for 5 min at 37° C in 4% paraformaldehyde. Cell suspensions were then permeabilized by incubating in PBS containing 0.1% Triton X-100 for 1 h on ice. For detection of BrdU incorporation, permeabilized cells were incubated for 10 min at 37°C in RPMI 1640 containing recombinant DNase. Afterward, suspensions were washed in incubated on ice for 40 min with anti-BrdU Abs following the manufacturer's protocol. Suspensions were washed and then incubated overnight with anti-FoxP3 Abs in PBS containing 0.5% BSA and analyzed the following day by flow cytometry. For FoxP3 staining only, the BrdU relevant steps were omitted.

Flow cytometric analysis

Simultaneous 8–10 color analyses of samples for intracellular FoxP3 and BrdU staining along with surface Ag expression were accomplished using a BD Biosciences LSR II flow cytometer using scatter properties to distinguish live and dead cells. For each individual experiment, software compensation of fluorescence overlap was calculated from singly stained controls using BD Biosciences FACSDiva software before sample acquisition. Data were subsequently analyzed using FlowJo software. In some cases, visualization of negative data acquired during 8–10 color analyses were facilitated by performing postacquisition biexponential transformations as previously described (24) using FlowJo software. Unless otherwise indicated, numbers in regions and quadrants of flow cytometry data represent the percentages of cells present. Detection of steady-state apoptosis using annexin-V and 7-AAD was conducted following the with the manufacturer's (BD Biosciences) protocol.

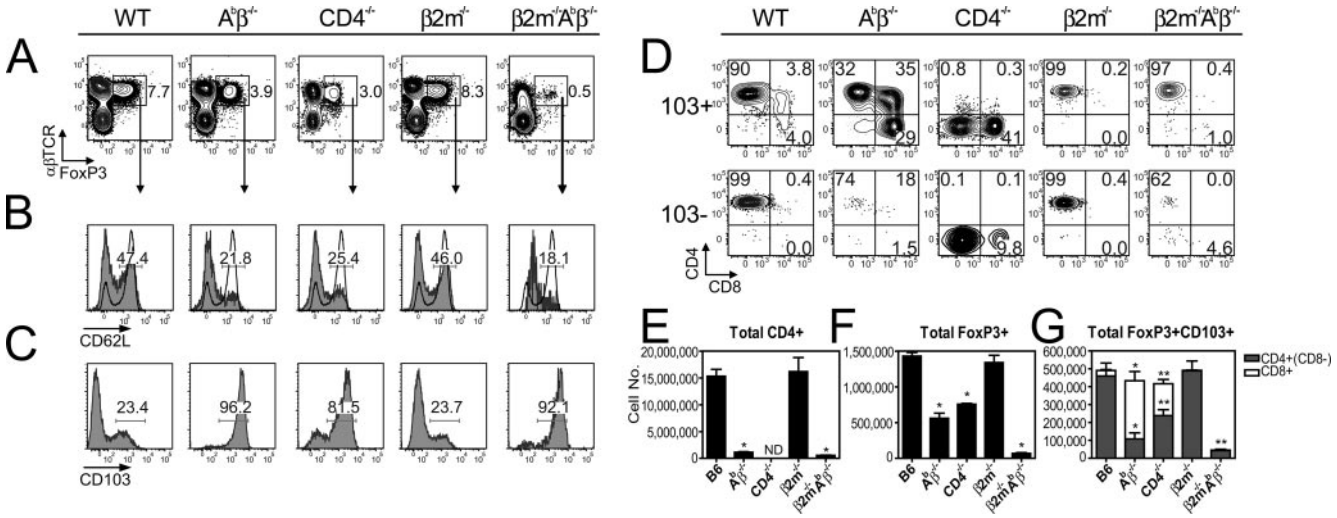

FIGURE 1. FoxP3$^+$ T cells with an effector/memory phenotype predominate in the absence of MHC class II-dependent T cell development. *A*, Expression of $\alpha\beta$TCR vs intracellular FoxP3 by total LN cells from the indicated strains of mice. *B*, Expression of CD62L (shaded histogram) or (*C*) CD103 by electronically gated $\alpha\beta$TCR$^+$FoxP3$^+$ populations shown above in *A*. In *B*, overlaid open histogram depicts CD62L expression on CD4$^+$FoxP3$^-$ cells and is included for reference. *D*, Expression of CD4 vs CD8 by CD103$^+$ (*top panels*) or CD103$^-$ (*bottom panels*) subsets gated as shown in *A*. Comparison of the average number of (*E*) total CD4$^+$, (*F*) total FoxP3$^+$, or (*G*) total CD103$^+$FoxP3$^+$ LN cells present in the various mouse strains. In *G*, closed and open regions indicate the proportion of FoxP3$^+$CD103$^+$ cells that express a CD4$^+$CD8$^-$ (CD4$^-$CD8$^-$ in the case of CD4$^{-/-}$ cells) or CD8 phenotype, respectively. Bar graphs in *E–G* illustrate the mean cell numbers calculated from flow cytometric analysis and are representative of three to five independent experiments. Bars indicate SE values (*, $p < 0.01$; **, $p < 0.05$).

Statistics

Where indicated, data were presented as mean ± SEM and significance was determined using GraphPad Prism software (GraphPad Software) by one-way ANOVA when comparing among multiple groups. For two group comparisons, the Student *t* test was used and a value of $p < 0.05$ was considered statistically significant.

Results

FoxP3$^+$ T cells with an effector phenotype predominate in MHC-deficient mice

We examined mouse strains lacking different MHC-encoded molecules for the presence of FoxP3$^+$ T cells in LNs. FoxP3-lineage cells are generally believed to be MHC class II-restricted and the frequency (Fig. 1*A*) and number (Fig. 1*F*) of FoxP3$^+$ T cells in β_2m$^{-/-}$ (MHC class I-deficient) mice appeared to confirm this notion. Nevertheless, a substantial population of peripheral TCR $\alpha\beta^+$FoxP3$^+$ T cells was also present in MHC class II-deficient mice (Fig. 1*A*). Although the absolute number of FoxP3$^+\alpha\beta^+$ T cells was reduced by roughly one-third compared with wild-type mice (Fig. 1*F*), this difference was less than the average 20-fold reduction in conventional CD4$^+$FoxP3$^-$ T cells that occurred in absence of MHC class II expression (Fig. 1*E*).

Whereas most FoxP3$^+$ T cells in wild-type and β_2m$^{-/-}$ strains appeared naive, expressing high levels of CD62L (Fig. 1*B*) and lacking expression of CD103 (Fig. 1*C*), those in A$^b\beta^{-/-}$ mice appeared to be activated, expressing low levels of CD62L (Fig. 1*B*) and high levels CD103 (Fig. 1*C*). A parallel analysis of CD4$^{-/-}$ mice, which also lack MHC class II-restricted T cells, demonstrated that a substantial population of FoxP3$^+$ T cells expressing an activated CD62L^{low}CD103$^+$ phenotype (Fig. 1, *B* and *C*) was present in numbers comparable to the A$^b\beta^{-/-}$ strain (Fig. 1, *A* and *F*). Mice lacking all conventional MHC class II-encoded genes (MHC II$^{\Delta/\Delta}$), and thus, devoid of unpaired MHC class II chains (22) also contained a substantial FoxP3$^+$ subset, indicating that such cells could develop in the complete absence of MHC class II expression (data not shown). Surprisingly, FoxP3$^+$ T cells could still be found, albeit in reduced numbers, in mice lacking both MHC class I and II (A$^b\beta^{-/-}\beta_2$m$^{-/-}$) expression (Fig. 1, *A* and *F*). These cells in A$^b\beta^{-/-}\beta_2$m$^{-/-}$ mice were all $\alpha\beta$TCR$^+$ and again uniformly displayed an activated CD62L^{low}CD103$^+$ phenotype (Fig. 1, *B* and *C*). The FoxP3$^+$ T cells in β_2m$^{-/-}$A$^b\beta^{-/-}$ mice demonstrated a diverse array of TCR Vβ chains suggesting they were polyclonal (data not shown).

The total number of effector CD103$^+$FoxP3$^+$ T cells in the A$^b\beta^{-/-}$ and CD4$^{-/-}$ strains was comparable to wild-type and β_2m$^{-/-}$ mice (Fig. 1*G*), but was reduced in β_2m$^{-/-}$A$^b\beta^{-/-}$ (Fig. 1*G*). The majority (~90%) of CD103$^+$FoxP3$^+$ T cells in wild-type mice expressed a CD4$^+$CD8$^-$ phenotype, with the remaining ~8–10% of CD103$^+$FoxP3$^+$ T cells split between the CD4$^+$CD8$^+$ and the CD4$^-$CD8$^+$ subsets, which were both found exclusively among the CD103$^+$ cells (Fig. 1*D*). A strikingly different pattern was observed in the A$^b\beta^{-/-}$ strain. In this study, CD103$^+$FoxP3$^+$ T cells were distributed roughly equally among the CD4$^+$CD8$^-$, CD4$^+$CD8$^+$, and CD4$^-$CD8$^+$ CD103$^+$FoxP3$^+$ subsets (Fig. 1*D*). The increased frequency of CD8$^+$FoxP3$^+$ T cells in A$^b\beta^{-/-}$ mice reflected an increase in absolute numbers and was not simply due to the decreased numbers of CD4$^+$FoxP3$^+$ T cells (Fig. 1*G*). Likewise, CD4$^{-/-}$ mice also contained a significantly increased CD8$^+$FoxP3$^+$ subset, accounting for roughly 50% of the total number of FoxP3$^+$ T cells (Fig. 1, *D* and *G*). The remainder of FoxP3-expressing T cells in CD4$^{-/-}$ mice was phenotypically CD8$^-$ (Fig. 1*D*). Thus, the absence of MHC class II-restricted FoxP3$^+$ T cells appeared to be accompanied by a compensatory increase in CD8-expressing FoxP3$^+$ subsets (Fig. 1, *D* and *G*). In contrast, the FoxP3$^+$ T cells in the A$^b\beta^{-/-}\beta_2$m$^{-/-}$ strain all expressed a CD4$^+$CD8$^-$ phenotype and completely lacked the CD4$^+$CD8$^+$ and CD4$^-$CD8$^+$ subsets found in β_2m-expressing strains. This result suggests that expression of CD8 by a FoxP3$^+$ T cell (regardless of coexpression of CD4) reflects MHC class I restriction. The loss of peripheral CD8$^+$FoxP3$^+$ T cells was also evident in K^b$^{-/-}$D^b$^{-/-}$ mice, indicating that the majority of CD8$^+$FoxP3$^+$ T cells are likely selected on conventional MHC class Ia molecules (G. L. Stephens, unpublished observation). In

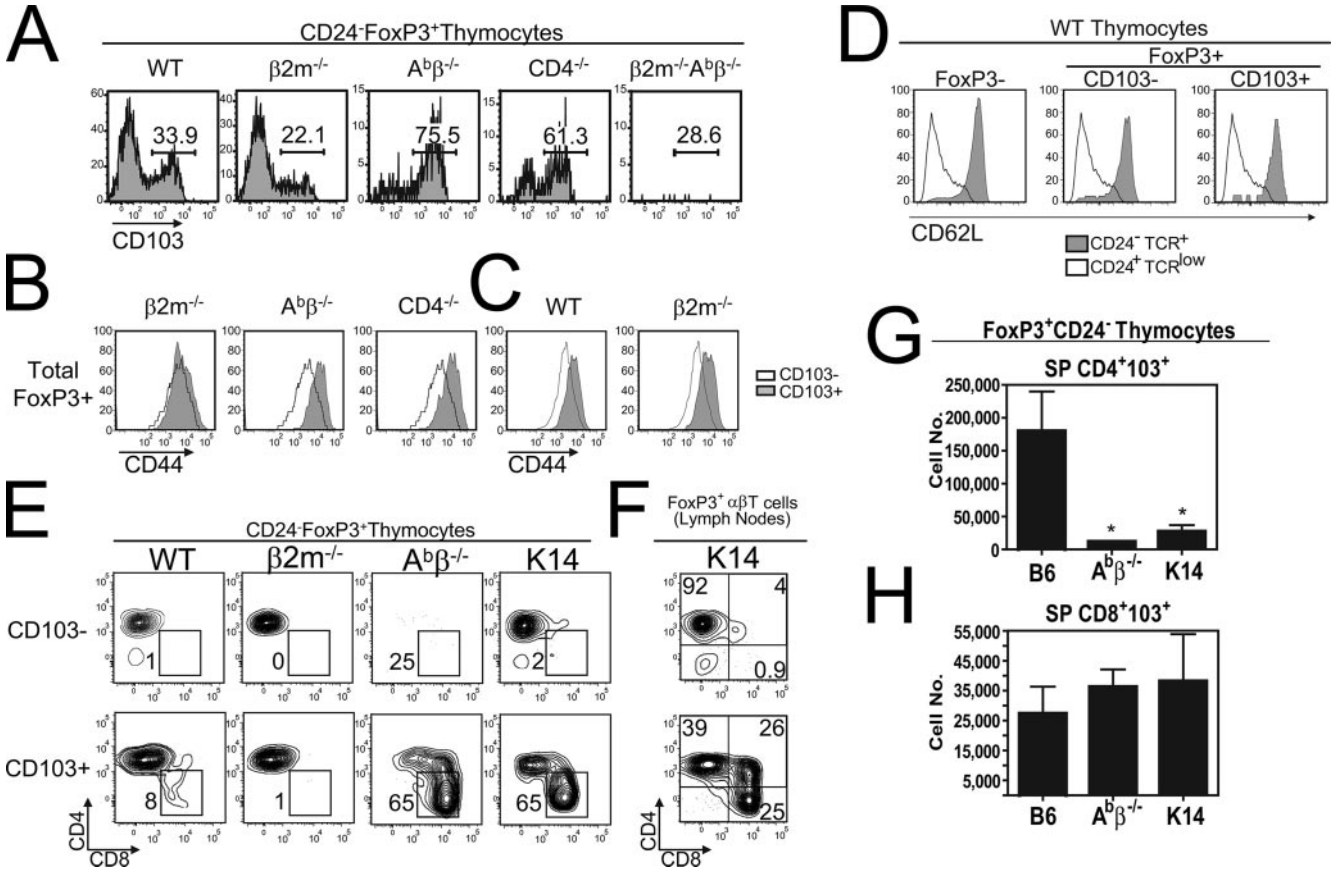

FIGURE 2. MHC class II expression by cortical thymic epithelium preferentially supports the intrathymic development of CD4$^+$FoxP3$^+$CD103$^-$ over CD4$^+$FoxP3$^+$CD103$^+$ T cells. *A*, Expression of CD103 or (*B*) CD44 among total CD24$^-$FoxP3$^+$ thymocytes is shown from the indicated strains of mice. In *B*, CD44 staining (closed histograms) is shown relative to the level on total CD24$^-$FoxP3$^+$ thymocytes in wild-type mice (open histogram). *C*, Expression of CD44 by CD103$^-$ (open histogram) or CD103$^+$ (closed histogram) subsets of CD24$^-$FoxP3$^+$ thymocytes from wild-type or β_2m$^{-/-}$ mice. *D*, Expression of CD62L among gated subsets of CD4$^+$ thymocytes from wild-type mice is shown overlaid upon its expression among immature CD4$^+$CD8$^+$ thymocytes. *E*, Profile of CD4 vs CD8 expression by CD103$^-$ (*top row*) or CD103$^+$ (*bottom row*) thymocyte subsets of mature FoxP3$^+$ thymocytes from the indicated mouse strains (*F*) or $\alpha\beta$TCR$^+$FoxP3$^+$ LN cells from K14 mice. *G*, A comparison of the average absolute number of mature (CD24$^-$) CD4$^+$CD8$^-$FoxP3$^+$CD103$^+$ or (*H*) CD4$^-$CD8$^+$FoxP3$^+$CD103$^+$ thymocytes present in wild-type, A$^b\beta^{-/-}$, and K14 mice. For flow cytometry data, numbers above regions or in quadrants indicate the percentage of cells present. Bars, SE values (*, $p < 0.01$) calculated from the percentages determined by flow cytometry as taken from at least three independent experiments.

contrast, CD4$^+$FoxP3$^+$ T cells could be found in all of the strains (excluding CD4$^{-/-}$ mice), irrespective of the expression of MHC proteins, suggesting that CD4 expression alone does not necessarily indicate MHC class II restriction for at least some FoxP3$^+$ T cells.

The development of a subset of effector FoxP3$^+$ T cells requires MHC expression by cells in the thymic medulla

Although most studies (25) suggest that FoxP3$^+$ regulatory T cells can develop via an intrathymic pathway, it was unclear whether the effector FoxP3$^+$ subset also developed in the thymus. We therefore evaluated mature (CD24$^-$) FoxP3$^+$ thymocytes for expression of the memory/activation markers CD44 and CD103. Approximately 15–20% of mature CD24$^-$FoxP3$^+$ thymocytes in wild-type and β_2m$^{-/-}$ mice expressed CD103 (Fig. 2*A*), whereas virtually all mature FoxP3$^+$ thymocytes in A$^b\beta^{-/-}$ mice, and the majority in the CD4$^{-/-}$ strain, expressed CD103 (Fig. 2*A*), as well as high levels of CD44 (Fig. 2*B*). Analysis of CD103$^+$FoxP3$^+$ thymocytes in wild-type and β_2m$^{-/-}$ mice revealed they also appeared more activated as they expressed high levels of CD44 (Fig. 2*C*). In contrast to LNs, no FoxP3$^+$ thymocytes of any kind were found in A$^b\beta^{-/-}\beta_2$m$^{-/-}$ mice (Fig. 2*A*), consistent with a previous study (19).

An exception to the pattern of activation markers expressed by effector FoxP3$^+$ thymocytes was CD62L. Whereas the majority of peripheral effector Foxp3$^+$ T cells lack expression of CD62L (13), those in the thymus expressed high levels of this marker (Fig. 2*D*). This difference between peripheral and thymic subsets suggests that effector FoxP3$^+$ thymocytes do not represent peripheral cells that have recirculated back to the thymus. Together, these results are consistent with the possibility that the effector phenotype expressed by the majority of peripheral FoxP3$^+$ T cells in A$^b\beta^{-/-}$ and CD4$^{-/-}$ mice, and by a subset of peripheral FoxP3$^+$ T cells in wild-type and β_2m$^{-/-}$ mice, is at least partially acquired because of an intrathymic developmental pathway. However, the absence of FoxP3$^+$ thymocytes in A$^b\beta^{-/-}\beta_2$m$^{-/-}$ mice suggests that a distinct pool of MHC-independent effector CD4$^+$FoxP3$^+$ T cells may potentially arise via an extrathymic developmental pathway.

Positive selection of conventional T cells requires low-avidity TCR interactions with peptide-MHC molecules expressed on thymic cortical epithelium. In contrast, the development of unconventional lineages of T cells often reflects a developmental program associated with positive selection by agonist ligands presented by hemopoietic cells (26). To determine whether the effector FoxP3$^+$ subset was selected on a cell type distinct from that promoting the development of naive Foxp3$^+$ T cells, we analyzed the thymus of

the K14 mouse strain, which expresses MHC class II exclusively on cortical thymic epithelium, but not on medullary epithelium or on bone marrow-derived cells (27). Although a previous study demonstrated the presence of functional $CD4^+CD25^+$ T cells in the K14 mouse, a characterization of naive and activated $FoxP3^+$ subsets has never been presented (17).

We compared the CD4/CD8 profile of effector and naive $FoxP3^+$ thymocytes in each of the different strains. In wild-type mice, the vast majority of effector $FoxP3^+$ thymocytes were phenotypically $CD4^+CD8^-$, although a smaller population expressing CD8 was also present (Fig. 2*E*, *bottom panels*). Virtually no $CD8^+$ cells were found among $CD103^-FoxP3^+$ thymocytes in either wild-type mice, nor in any of the other mouse strains examined (Fig. 2*E*, *top panels*). Although $\beta_2m^{-/-}$ mice contained many mature $CD4^+CD8^-FoxP3^+$ thymocytes in both effector and naive compartments, subsets expressing CD8 were not detectable (Fig. 2*E*). In $A^b\beta^{-/-}$ mice, mature $FoxP3^+$ thymocytes were found primarily among the $CD8^+CD103^+$ subsets (Fig. 2*E*, *bottom panel*) and were essentially undetectable within the $CD103^-$ compartment (Fig. 2*E*, *top panel*).

In the K14 thymus, we found that expression of MHC class II exclusively on cortical thymic epithelium allowed the selection of naive $CD4^+CD8^-FoxP3^+$ thymocytes (Fig. 2*E*, *top panel*). In contrast, the selection of effector $CD4^+CD8^-FoxP3^+$ thymocytes was strikingly diminished in K14 mice, where the CD4/CD8 profile appeared much more similar to the $A^b\beta^{-/-}$ strain than to that of wild-type mice (Fig. 2*E*, *bottom panel*). This was also reflected in the absolute numbers, which were significantly diminished to a similar extent in K14 and $A^b\beta^{-/-}$ strains relative to controls (Fig. 2*G*). Conversely, the increased frequency of $CD8^+FoxP3^+$ thymocytes in K14 and $A^b\beta^{-/-}$ mice (Fig. 2*E*, *bottom panel*) was not due to changes in absolute cell numbers, which were not significantly altered compared with wild-type mice (Fig. 2*H*). The peripheral LNs of K14 mice also resembled the $A^b\beta^{-/-}$ strain (Fig. 1*D*, *top panel*) in terms of the distribution of effector $FoxP3^+$ subsets, where a compensatory increase in $CD103^+CD8^+FoxP3^+$ T cells was also apparent (Fig. 2*F*, *bottom panel*). However, K14 mice clearly differed from the $A^b\beta^{-/-}$ strain in that they contained a substantial population of phenotypically naive peripheral $CD103^-CD4^+CD8^-FoxP3^+$ T cells (Fig. 2*E*, *top panel*). Thus, MHC expression by cortical thymic epithelium can efficiently select naive phenotype $FoxP3^+$ T cells, while the development of a portion of the effector $CD4^+FoxP3^+$ subset requires interactions with MHC molecules expressed by cells in the thymic medulla.

Effector-phenotype $FoxP3^+$ T cells are enriched in proliferating cells

The increased expression of activation/memory markers by effector $FoxP3^+$ T cells, and the compensatory expansion of the $CD8^+FoxP3^+$ subsets in mice lacking MHC class II expression in the thymic medulla, led us to evaluate the relative proliferation rates of these different subsets. We assessed the steady-state proliferation of peripheral $CD25^+$ T cells in wild-type, $\beta_2m^{-/-}$, and $A^b\beta^{-/-}$ mice using the nucleoside thymidine analog BrdU, which is rapidly incorporated into the DNA of proliferating cells. Staining of LN cells harvested from mice injected the previous day with BrdU revealed that the effector $CD25^+CD103^+$ subset in wild-type and $\beta_2m^{-/-}$ mice contained roughly 3- to 4-fold more proliferating cells (Fig. 3*A*) than the naive $CD103^-CD25^+$ T cell compartment. Similar results were obtained in $A^b\beta^{-/-}$ mice, where the steady-state proliferation of total $CD4^+CD8^-CD25^+$ and $CD8^+CD25^+$ subsets was comparable to that of the effector $CD25^+$ subset in wild-type mice (Fig. 3*B*). This latter observation

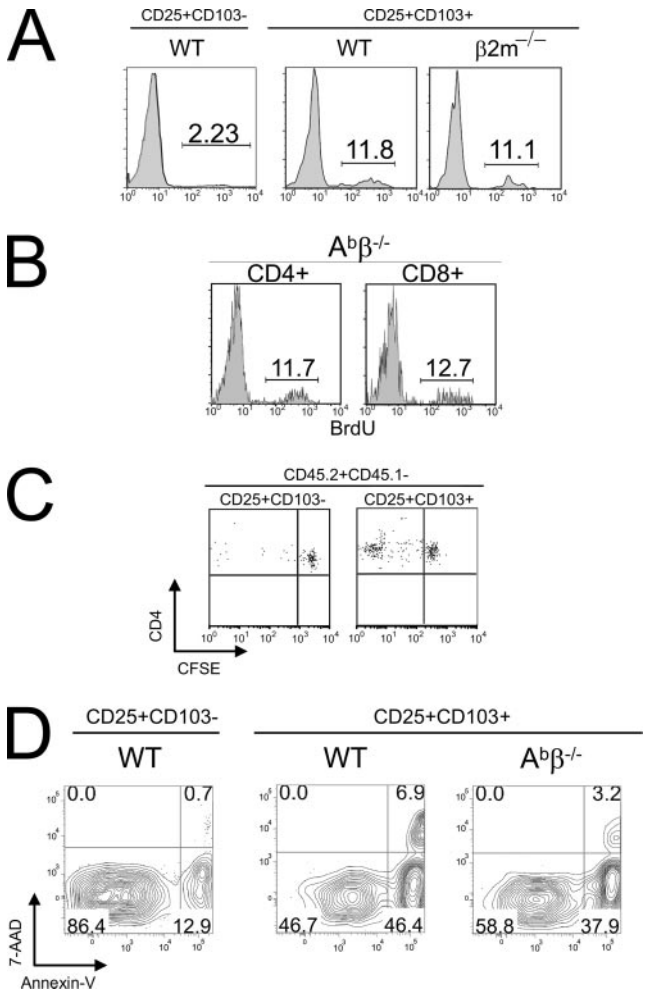

FIGURE 3. The effector $CD25^+$ subset is enriched in proliferating cells. *A*, Steady-state proliferation of endogenous $CD25^+$ T cells in C57BL/6 mice i.v. injected with 1 mg of BrdU 16 h before sacrifice. BrdU incorporation by either total wild-type $CD4^+CD25^+$ T cells (*leftmost histogram*) or within the $CD103^+$ subset from wild-type (*middle*) or $\beta_2m^{-/-}$ (*right*) mice. *B*, BrdU incorporation by total $CD4^+CD8^-CD25^+$ (*left*) and $CD8^+CD25^+$ (*right*) T cells from MHC class II ($A^b\beta^{-/-}$) deficient mice. *C*, Detection of CFSE dilution after 7 days by donor CD103-depleted (*left plot*) or total $CD4^+CD25^+$ T cells (*right dot plot*) purified from $CD45.2^+$ mice following transfer into congenic CD45.1-expressing wild-type hosts. *D*, Steady-state apoptosis among $CD25^+$ subsets in wild-type (*left* and *middle plots*) or $A^b\beta^{-/-}$ mice (*right plot*) from freshly isolated LN suspensions was determined by staining with annexin-V and 7-AAD. For flow cytometry data, numbers above regions or in quadrants indicate the percentage of cells present. Results are representative of two to four independent experiments.

was consistent with the effector phenotype expressed by the vast majority (~90%) of $FoxP3^+$ T cells present in $A^b\beta^{-/-}$ mice.

The relative contribution of the $CD103^+$ subset to the overall proliferation observed within the $CD4^+CD25^+$ T cell compartment was further evaluated by assessing the dilution of CFSE by purified total $CD4^+CD25^+$ and CD103-depleted $CD4^+CD25^+$ T cells from wild-type mice following adoptive transfer into intact congenic recipients. After 7 days, suspensions from recipient LNs were stained for surface Ags and intracellular FoxP3. Consistent with the BrdU-labeling studies, the depletion of $CD103^+$ cells from the total donor $CD4^+CD25^+$ T cell population led to a marked attenuation in the frequency of CFSE low cells (Fig. 3*C*). These results further support the notion that the $CD103^+$ subset,

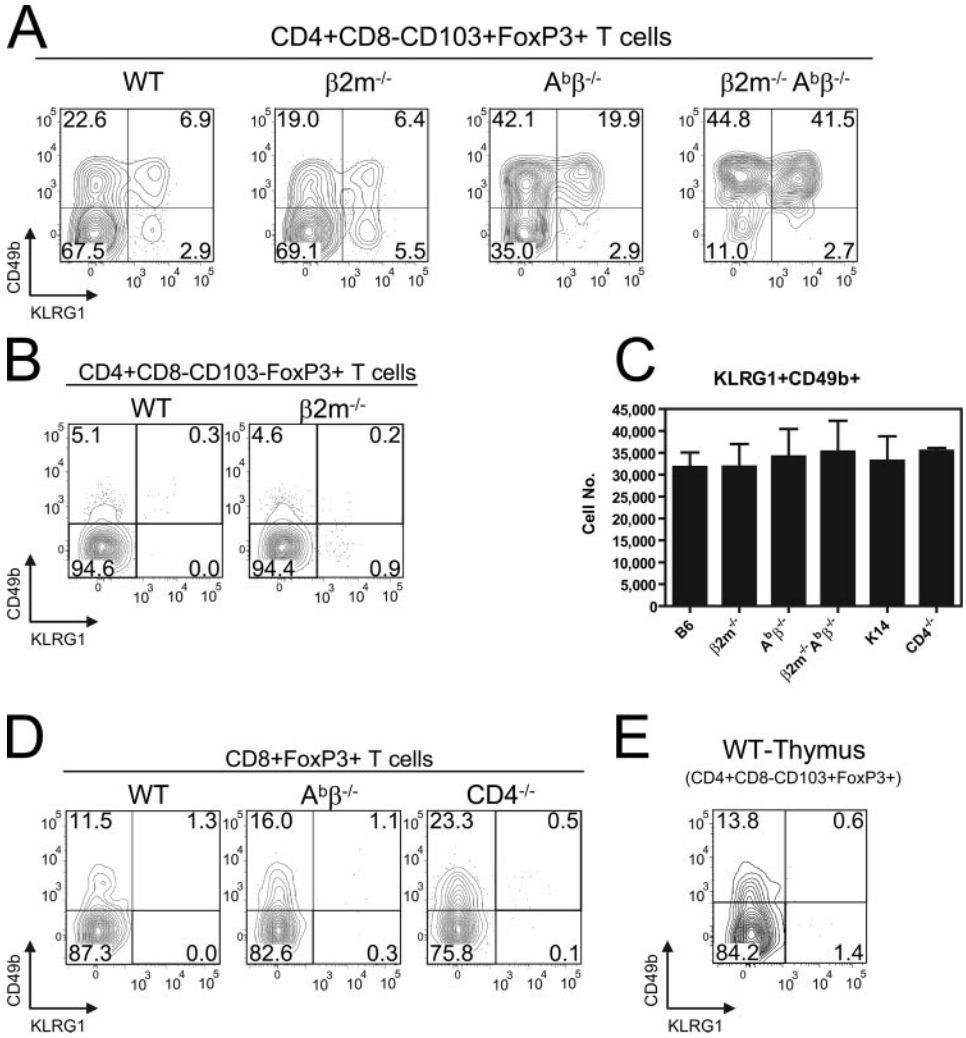

FIGURE 4. Expression of NK markers by subsets of activated FoxP3$^+$ T cells in MHC-deficient mouse strains. *A*, Expression of the NK markers CD49b and KLRG1 by CD103$^+$FoxP3$^+$ subsets. Single-cell suspensions from LNs harvested from the indicated mouse strains were surface stained with Abs specific for CD4, CD8, CD103, CD49b, and KLRG1 followed by intracellular staining to detect FoxP3. *B*, Expression of CD49b vs KLRG1 on electronically gated FoxP3$^+$ CD103$^-$ T cells from wild-type (*left*) or β_2m$^{-/-}$ mice (*right*). *C*, Average numbers of KLRG1$^+$CD49b$^+$FoxP3$^+$ T cells found in various transgenic and knockout mouse strains calculated from analysis of flow cytometric data. *D*, Expression of CD49b vs KLRG1 on electronically gated CD8$^+$FoxP3$^+$ T cells from the indicated strains or (*E*) among gated CD4$^+$CD103$^+$FoxP3$^+$ thymocytes from wild-type mice. Bars in *C* indicate SE values. Representative results from at least two independent experiments.

which includes the majority of effector FoxP3$^+$ T cells, substantially contributes to the spontaneous proliferation exhibited by CD25$^+$FoxP3$^+$ T cells in vivo.

As the number of CD103$^+$CD25$^+$ cells remains relatively stable during the first 6 mo of life (G. L. Stephens, unpublished observations), it seemed likely that the high constitutive proliferation rate of the effector FoxP3$^+$ subset was accompanied by a correspondingly high rate of death. A comparison of the frequency of apoptotic cells present in the effector vs naive phenotype CD25$^+$ T pool was determined by staining freshly isolated cells for cell surface Ags in combination with annexin V and 7-AAD. A significantly higher proportion of cells within the effector CD25$^+$CD103$^+$ subset displayed signs of apoptosis compared with naive CD103$^-$ T cells in the same animal (Fig. 3*D*). Effector CD25$^+$CD103$^+$ populations in A$^b\beta^{-/-}$ mice also contained a high proportion of apoptotic cells (Fig. 3*D*). Together, these studies suggest that a fine balance between proliferation and death regulates the size of the effector FoxP3$^+$ T cell compartment in the steady state.

Differential expression of NK cell-associated markers distinguishes MHC-dependent from MHC-independent FoxP3$^+$CD103$^+$ T cells

The presence of effector Foxp3$^+$ T cells only in the peripheral lymphoid tissues of A$^b\beta^{-/-}\beta_2$m$^{-/-}$ mice suggested a thymic-independent origin. To further characterize this subset, we examined several markers expressed by other types of unconventional T cell lineages. Two cell surface Ags, both previously associated with NK cells, further subdivided the effector FoxP3$^+$ subset. CD49b is considered a pan-NK cell marker, although it is expressed by T cells, particularly those of the invariant NK T cell lineage (28, 29). KLRG1 has been mostly characterized on subsets of NK cells, but a link between KLRG1 and FoxP3$^+$ T cells was suggested from microarray studies. In these studies, KLRG1 expression was associated with FoxP3$^+$ subsets that exhibit spontaneous in vivo proliferation (19) and a preferential localization in inflamed tissues (30, 31).

An analysis of Foxp3$^+$ LN T cells revealed that expression of CD49b and KLRG1 was largely confined to CD103$^+$FoxP3$^+$ cells (Fig. 4*A*), which expressed these markers at a substantially higher frequency than their CD103$^-$ counterparts (Fig. 4*B*). In wild-type and β_2m$^{-/-}$ strains, ~25–30% of CD4$^+$FoxP3$^+$CD103$^+$ T cells expressed CD49b and among those, roughly one-third coexpressed KLRG1 (Fig. 4*A*). An increased proportion (50–60%) of effector CD4$^+$FoxP3$^+$ T cells in A$^b\beta^{-/-}$ mice expressed CD49b, and approximately one-third of these CD49b$^+$ cells coexpressed KLRG1 (Fig. 4*A*). In β_2m$^{-/-}$A$^b\beta^{-/-}$ mice, where 85–90% of total FoxP3$^+$ T cells expressed CD49b, roughly half of the FoxP3$^+$ cells also coexpressed KLRG1 (Fig. 4*A*). Although both A$^b\beta^{-/-}$ and A$^b\beta^{-/-}\beta_2$m$^{-/-}$ strains displayed an increased frequency of FoxP3$^+$ CD49b$^+$KLRG1$^+$ T cells, absolute numbers were similar in all of the strains examined (Fig. 4*C*). The CD49b$^+$KLRG1$^+$ subset of FoxP3$^+$ T cells was present exclusively within the

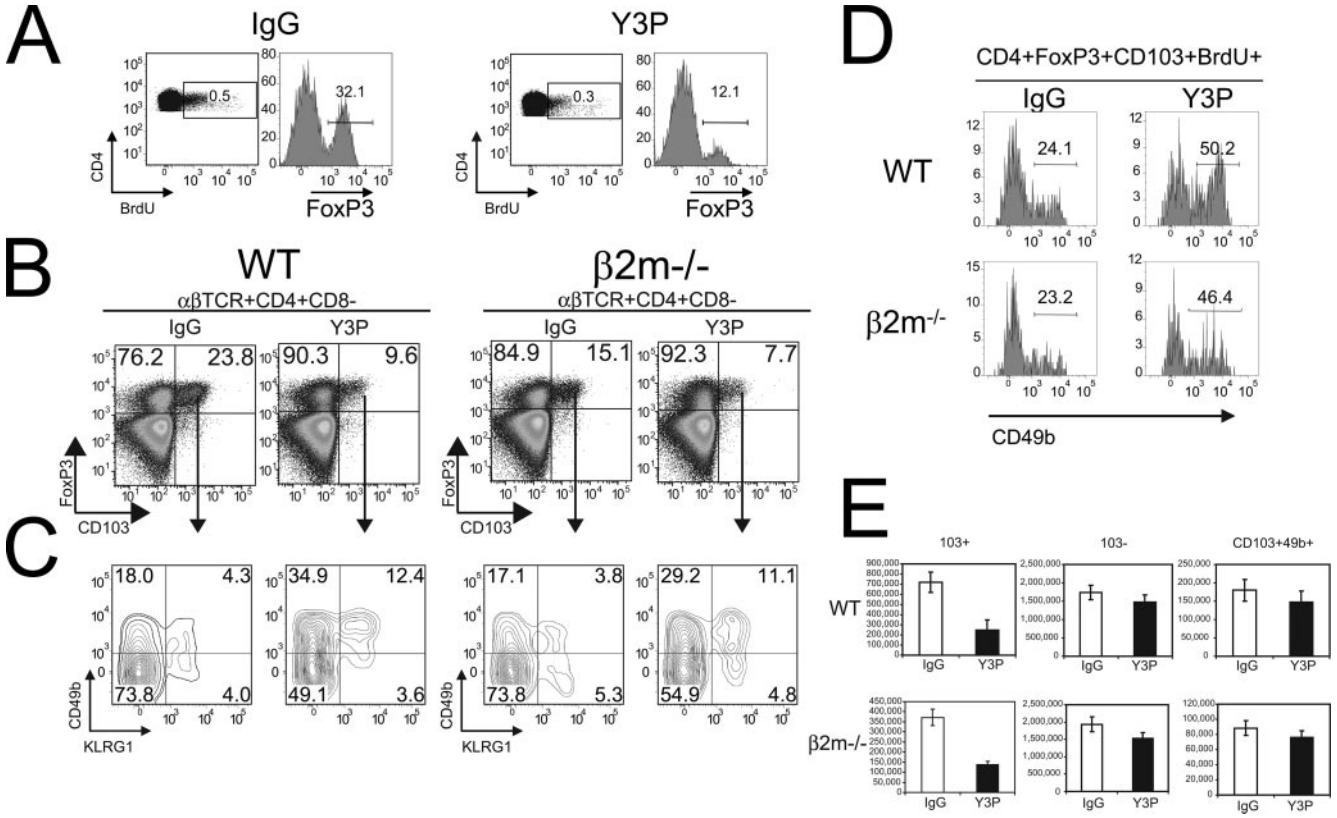

FIGURE 5. Acute blockade of MHC class II molecules leads to depletion of the FoxP3$^+$CD103$^+$ T cell compartment in both wild-type and MHC class I-deficient mice. *A*, Incorporation of BrdU by wild-type CD4$^+$ T cells in mice treated every other day with 2 mg/mouse control (IgG; *left*) or anti-MHC class II specific Abs (Y3P; *right*). Histograms depict the expression of FoxP3 by gated CD4$^+$BrdU$^+$ T cells. *B*, *Upper dot plots*, Expression of FoxP3 vs CD103 on $\alpha\beta$TCR$^+$CD4$^+$CD8$^-$ gated cells. Percentages indicate the frequencies of CD103$^+$ or CD103$^-$ T cells among the FoxP3$^+$ population. Histograms below the dot plots illustrate the expression of CD49b vs KLRG1 among FoxP3$^+$CD103$^+$ subsets as shown by the respective arrows. *D*, The frequency of CD49b$^+$ T cells among the indicated subset of BrdU$^+$ cells present in wild-type or β_2m$^{-/-}$ mice treated as described in *A*. *E*, Absolute numbers of the indicated FoxP3$^+$ subsets in wild-type (*top panels*) and β_2m$^{-/-}$ (*bottom panels*) mice treated as described in *A*. Results are representative of three independent experiments. Bars indicate SE values ($*$, $p < 0.05$) calculated from the percentages determined by flow cytometry.

CD4$^+$FoxP3$^+$ compartment, as coexpression of these markers by CD8$^+$FoxP3$^+$ T cells in both wild-type and A$^b\beta^{-/-}$ mice was essentially undetectable (Fig. 4*D*). CD49b$^+$KLRG1$^+$-expressing T cells could also not be found among conventional FoxP3$^-$CD4$^+$ (data not shown) or CD8$^+$ (data not shown) T cells. Importantly, although a minor fraction expressing a CD49b$^+$KLRG1$^-$FoxP3$^+$ phenotype was observed, effector CD103$^+$FoxP3$^+$ cells coexpressing CD49b and KLRG1 were not detectable in the thymus of wild-type animals (Fig. 4*E*), which is consistent with the absence of detectable FoxP3$^+$ thymocytes in A$^b\beta^{-/-}\beta_2$m$^{-/-}$ mice. Confirming a previous study (19), expression of NK1.1 by FoxP3$^+$ T cells could not be detected in parallel analyses by flow cytometry (data not shown). Thus, coexpression of CD49b and KLRG1 identifies a unique subset of FoxP3$^+$ regulatory T cells, which is the dominant FoxP3$^+$ population in mice lacking expression of MHC class I and II.

Preferential depletion of CD49b$^-$CD103$^+$FoxP3$^+$ T cells in vivo following acute blockade of MHC class II/TCR interactions

To further determine whether the CD103$^+$CD49b$^+$KLRG1$^{+/-}$ subset present in wild-type animals also represented an MHC-independent population, we examined whether the steady-state proliferation of effector-phenotype FoxP3$^+$ T cells required recognition of cognate-MHC molecules in vivo. Wild-type mice were treated during the preceding 4 days with a blocking Abs specific for MHC class II molecules and then received a single i.v. pulse of BrdU. The next day, LNs were harvested and incorporation of BrdU was determined by multiparameter flow cytometry. In control-treated animals, FoxP3$^+$ cells accounted for ~30% of the CD4$^+$ T cells that incorporated BrdU (Fig. 5*A*, *left panel*). Following acute blockade of MHC class II, this frequency was reduced, although some proliferating FoxP3$^+$ T cells remained (Fig. 5*A*, *right panel*). Blockade of TCR/MHC class II interactions led to a comparable reduction in the frequency of CD4$^+$ cells expressing FoxP3$^+$ and CD103$^+$ in both wild-type and β_2m$^{-/-}$strains (Fig. 5*B*), but anti-MHC class II-treated mice had increased frequencies of both the CD49b$^+$KLRG1$^+$ and CD49b$^+$KLRG1$^-$ subsets (Fig. 5*C*). The majority of effector FoxP3$^+$ T cells incorporating BrdU following MHC class II blockade in both wild-type and β_2m$^{-/-}$ mice expressed CD49b (Fig. 5*D*, *right histograms*), while only ~25% of dividing cells were CD49b$^+$ in the control-treated animals (Fig. 5*D*, *left panel*). Blocking MHC class II had little impact on the number of FoxP3$^+$CD103$^+$ cells within both CD49b$^+$ subsets in the two mouse strains (Fig. 5*E*). Thus, blockade of MHC class II in both wild-type and MHC class I-deficient mice led to the preferential depletion of the CD49$^-$ subset with a corresponding enrichment in the CD49$^+$ subset of CD103$^+$FoxP3$^+$ T cells. Taken together, these data are consistent with the possibility that the CD49b$^+$ subset present in wild-type mice is enriched with proliferating MHC-independent FoxP3$^+$ T cells.

CD103$^+$FoxP3$^+$ T cells exert Ag-nonspecific suppression directly ex vivo irrespective of their MHC restriction

FoxP3$^+$ regulatory T cells require TCR-mediated signals to activate their suppressive functions (32). Ligation of the TCR does not induce proliferation of CD4$^+$FoxP3$^+$ T cells in vitro in the absence of exogenous γ-chain cytokines (32, 33). However, in vivo, Foxp3$^+$ T cells proliferate upon encounter with cognate Ag (34–36). The identification of a proliferating FoxP3$^+$ T cell subset in vivo led us to hypothesize that these cells were being continuously activated and, thus, could potentially exert Ag-nonspecific suppression of CD4$^+$CD25$^-$ responder T cell proliferation directly ex vivo without the need for exogenous TCR stimulation. To test this possibility, coculture suppression assays were performed using sort-purified CD103$^+$ and CD103$^-$ CD4$^+$CD25$^+$ T cell subsets from nonimmunized wild-type mice. These populations were evaluated for their respective capacity to exert Ag-nonspecific suppression of HA-peptide specific TCR-transgenic CD4$^+$CD25$^-$ T cells. CD25$^+$CD103$^-$ and CD25$^+$CD103$^+$ subsets both suppressed the proliferation of HA-specific CD4$^+$CD25$^-$ T cells when soluble anti-CD3 Abs were used as a polyclonal stimulator (Fig. 6*A*, *left*). However, when HA peptide was used to specifically stimulate CD4$^+$CD25$^-$ responder T cells, only the CD103$^+$ subset was capable of suppressing proliferation directly ex vivo (Fig. 6*A*, *right*). The suppression mediated by the CD103$^+$ subset was not dependent upon the production of IL-10 or TGFβ, as neutralization of both cytokines in cocultures had no effect on the observed suppression (data not shown). The ability of the CD103$^+$ subset to suppress T cell responses directly ex vivo coincided with an increased basal level of FoxP3 (data not shown).

A previous study suggested an absolute requirement for MHC class II expression in the generation of functional regulatory CD4$^+$CD25$^+$ T cells based on the observation that total CD4$^+$CD25$^+$ T cells from A$^b\beta^{-/-}$ mice lacked suppressor function (17). Thus, the ability of the effector CD4$^+$CD8$^-$FoxP3$^+$ subset in MHC class II-deficient animals to regulate T cell responses was uncertain. In the presence of soluble anti-CD3, CD25$^+$CD103$^+$ T cells from A$^b\beta^{-/-}$ mice suppressed responder CD4$^+$CD25$^-$ T cell proliferation (Fig. 6*B*, *left*) and inhibited the HA response comparably to wild-type CD25$^+$CD103$^+$ T cells. In contrast, the addition of CD25$^+$CD103$^-$ T cells enhanced the response to anti-CD3 and failed to block the HA response (Fig. 6*B*, *right*) suggesting they were activated effector cells. Similarly, CD4$^+$CD25$^+$CD103$^+$ purified from A$^b\beta^{-/-}\beta_2m^{-/-}$ mice also demonstrated a capacity to suppress both the response to soluble anti-CD3 Abs and HA peptide (Fig. 6*C*), analogous to their wild-type and A$^b\beta^{-/-}$ counterparts.

Lastly, we examined the suppressive activity of the effector CD4$^+$CD25$^+$ T cells that remained following acute MHC class II blockade. Consistent with the potential MHC independence of this subset, treatment with anti-MHC class II Abs did not hamper the suppressive activities of the CD103$^+$ T cells that remained following this treatment (Fig. 6*D*). The ability of CD103$^+$CD25$^+$ cells to suppress directly ex vivo was not a consequence of a costimulatory signal delivered by cross-linking of CD103 by the CD103 Abs used for sort purification (37), as the KLRG1$^+$ subset of CD25$^+$ T cells, which uniformly expresses CD103, also suppressed HA peptide-specific responses directly ex vivo (data not shown). These results suggest that the observed suppressive activity of effector CD25$^+$CD103$^+$ T cells is an intrinsic property, rather a consequence of the inadvertent activation due to the purification method used. The ability of effector FoxP3$^+$ T cells to exhibit suppressor/effector capacity directly ex vivo further contrasts them with the naive FoxP3$^+$ subset, thus supporting the notion that the former may have been activated in vivo.

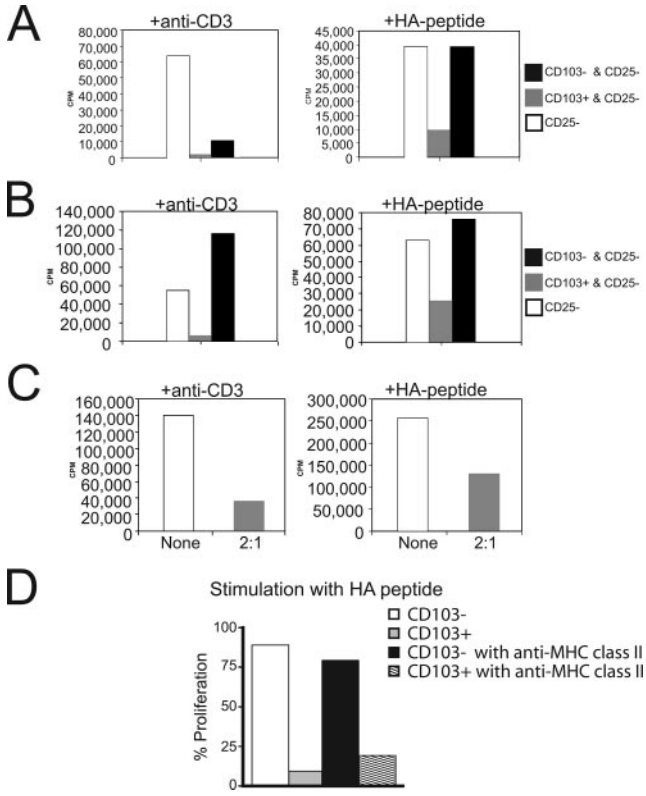

FIGURE 6. Ex vivo suppressive capacities of freshly isolated CD25$^+$FoxP3$^+$ T cells from MHC-deficient mouse strains. *A*, CD103$^+$ and CD103$^-$ CD4$^+$CD25$^+$ T cells from wild-type mice were cocultured with HA-specific TCR-transgenic CD4$^+$CD25$^-$ responder cells (5×10^4 well) in the presence of soluble anti-CD3 (0.5 μg/ml; *left graph*) or HA-peptide (16 μM; *right graph*) along with T cell-depleted irradiated splenocytes (5×10^4/well). Cultures were pulsed with [^{3}H]thymidine for the last 6–8 h of the 72-h culture period. *B*, Performed as in *A* using FACS-purified CD4$^+$CD25$^+$CD103$^+$ and CD4$^+$CD25$^+$CD103$^-$ T cells from A$^b\beta^{-/-}$ mice. *C*, Cocultures assays were performed as in *A* with CD4$^+$CD25$^+$CD103$^+$ T cells sort purified from A$^b\beta^{-/-}\beta_2m^{-/-}$ mice. Ratio below the graph indicates the relative proportion of responders to suppressors. *D*, Polyclonal CD103$^+$ and CD103$^-$ subsets of CD4$^+$CD25$^+$ T cells (50,000/well) purified by FACS from mice treated with isotype control or MHC class II-specific Abs were cocultured as outlined in *A*. Results are presented as a percentage of the proliferation of CD4$^+$CD25$^-$ T cells cultured alone. Data are presented as the mean values calculated from triplicate wells and are representative of between two and four independent experiments.

Effector FoxP3$^+$ T cells are enriched within inflammatory sites

We next compared effector and naive FoxP3$^+$ T cells for their relative ability to participate acutely during immune regulation in vivo by monitoring the composition of both subsets in draining and nondraining LNs following the injection of the TLR4 agonist LPS. The frequency of total FoxP3$^+$ T cells within the CD4$^+$ compartment was not dramatically altered in the draining vs nondraining nodes 5 days after LPS injection (Fig. 7*A*). However, further analysis of FoxP3$^+$ subsets revealed that effector CD103$^+$FoxP3$^+$ T cells became the dominant population in draining LNs where they were increased in frequency by 2-fold (Fig. 7*B*, *bottom panel*). This was not reflective of an overall increase but was limited to the draining lymphoid tissues; the frequency of effector FoxP3$^+$ T cells present in nondraining LNs was largely unchanged and appeared similar to that of unmanipulated mice (Fig. 7*B*, *top plot*). Among the FoxP3$^+$CD103$^+$ T cells in the draining LNs, a further enrichment of KLRG1$^+$CD49b$^+$ T cells was also readily apparent (Fig. 7*C*). Analysis of absolute cell numbers revealed that

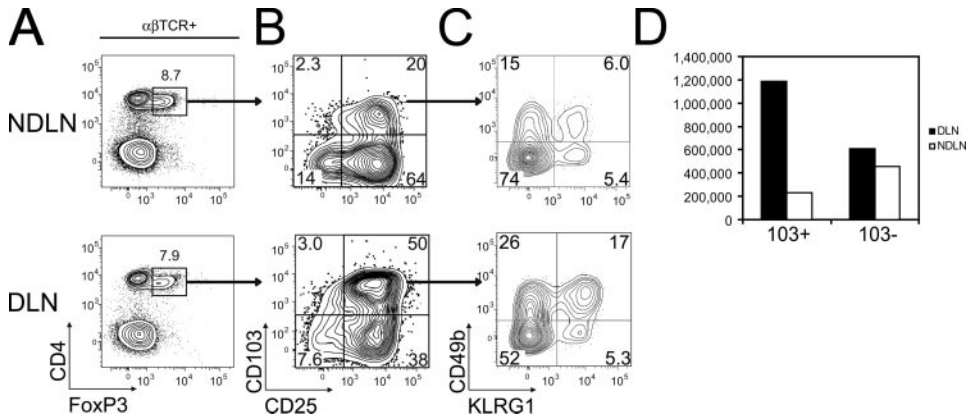

FIGURE 7. Enrichment in effector FoxP3$^+$CD103$^+$ T cells is observed in lymphoid tissues draining an inflammatory site. *A*, Dot plots show staining of CD4 vs FoxP3 on electronically gated $\alpha\beta$TCR$^+$ cells present in nondraining (*top panels*; NDLN) or draining (*bottom panels*; DLN) LNs from wild-type mice injected s.c. 5 days earlier with 100 μg of LPS. *B*, Expression of CD103 and CD25 by the CD4$^+$FoxP3$^+$ subset gated depicted in *A* present in the nondraining (*top*) or draining (*bottom*) LNs. *C*, CD49b vs KLRG1 expression by CD103$^+$CD25$^+$ T cells shown in *B* present in the nondraining (*top*) or draining (*bottom*) LNs. *D*, Absolute number of effector FoxP3$^+$ T cells found in the draining (■) vs nondraining (□) LNs calculated from percentages determined by flow cytometry. Results are representative of three independent experiments.

FoxP3$^+$CD103$^+$ T cells were increased by roughly 5-fold in the draining LNs (Fig. 7*D*). Thus, s.c.-injected LPS is alone sufficient to result in the enrichment of effector FoxP3$^+$ T subsets in the draining LNs.

Discussion

We have analyzed in depth the role of the MHC in the development of Foxp3$^+$ T cells and correlated the phenotypic properties of Foxp3$^+$ T cells developing in MHC-deficient mice with their expression of cell surface Ags and function both in vitro and in vivo. In addition to the conventional MHC class II-restricted Foxp3$^+$ population, we have identified a major population thymic-derived effector Foxp3$^+$CD8$^+$ T cells that are MHC class I restricted in mice lacking MHC class II Ags and a population of thymic-independent peripheral effector CD4$^+$Foxp3$^+$ T cells present in mice lacking all conventional MHC Ags. Most effector CD4$^+$Foxp3$^+$ T cells in wild-type mice are thymic derived although some are likely to be thymic independent. Although distinct from one another in their requirements for classical MHC molecules and in their thymic origin, the effector FoxP3$^+$ subsets described here share several common features that closely parallel those described for other types of unconventional T cells. These include constitutive effector activity, an activated cell surface phenotype, and the propensity to rapidly localize to inflamed lymphoid organs or tissues. We reason that effector FoxP3$^+$ T cells may play a specialized role during the early stages of an immune response perhaps by acting during the priming phase as an initial means to modulate the adaptive T cell response.

One of the most striking findings in our study was the identification of large numbers of thymic-derived CD4$^-$CD8$^+$ and CD4$^+$CD8$^+$ Foxp3$^+$ T cells in the periphery of mice lacking MHC class II Ags, while very few of either of these populations can be identified in normal mice. A model consistent with this result is that the thymic-derived effector FoxP3$^+$ T cell subsets restricted to conventional MHC class I and II Ags compete for limited resources under steady-state conditions in vivo. Such competition may play a role in maintaining the steady-state size of this compartment at a relatively constant level over the lifetime of the animal. In A$^b\beta^{-/}$, K14, and wild-type strains, we found that the absolute number of CD8$^+$FoxP3$^+$ thymocytes was comparable, suggesting that alterations in thymic selection were not responsible for the expanded CD8$^+$FoxP3$^+$ populations. Rather, our data suggest that the relative abundance of CD8$^+$FoxP3$^+$ T cells in MHC class II$^{-/-}$ mice was related to the intrinsic capacity of effector FoxP3$^+$ T cells to fill the void left by the absence of MHC class II-restricted T cells. This conclusion was further supported by the observation that the CD8$^+$FoxP3$^+$ population in MHC class II$^{-/-}$ mice undergoes extensive steady-state proliferation in vivo, similar to effector CD4$^+$CD103$^+$FoxP3$^+$ T cells in normal mice. Thus, in the absence of competition from MHC class II-restricted effector FoxP3$^+$ T cells, the CD8$^+$FoxP3$^+$ subset is allowed to emerge as a dominant population. In contrast to their MHC-restricted counterparts, our results demonstrated that the effector MHC-independent FoxP3$^+$ subset in the β_2m$^{-/-}$A$^b\beta^{-/-}$ mice did not expand to fill the void left by the absence of MHC-restricted effector FoxP3$^+$ subsets. In fact, their absolute numbers were surprisingly conserved in all of the strains examined. This leads us to speculate that the MHC-independent FoxP3$^+$ subset may occupy a niche that is distinct from that of MHC-restricted effector FoxP3$^+$ T cells.

In wild-type mice, the proportion of CD4$^+$Foxp3$^+$CD103$^+$ effector T cells in the thymus closely paralleled the proportion of these cells in the periphery (~20–30% of Foxp3$^+$ cells). This finding raised the possibility that the naive and effector subsets might be the products of distinct development pathways in the thymus. One intriguing observation consistent with this hypothesis is that the K14 strain, which lacks MHC class II-restricted effector FoxP3$^+$ T cells in both the thymus and peripheral lymphoid tissues, still maintains a substantial population of naive CD4$^+$ FoxP3$^+$ cells but has diminished numbers of CD4$^+$CD8$^-$CD103$^+$ FoxP3$^+$ cells. This result implies that the thymic selection of effector FoxP3$^+$ T cells is dependent upon interactions with APCs present exclusively in the medullary region of the thymus. Furthermore, the presence of naive CD4$^+$CD103$^-$FoxP3$^+$ T cells in K14 mice had no effect on the expansion of the effector CD8$^+$ FoxP3$^+$ T subset, thus supporting the notion that competition for a unique niche likely occurs exclusively among the effector FoxP3$^+$ subsets.

The demonstration that CD49b is expressed by a substantial portion of effector FoxP3$^+$ T cells is somewhat surprising given its association with invariant NKT cells, which have been shown in some contexts to possess immunoregulatory functions. An earlier study demonstrated that CD4$^+$CD49b$^+$ T cells were superior to CD4$^+$CD25$^+$ T cells in their ability to suppress the onset of diabetes following their adoptive transfer into BDC2.5 TCR Tg

Rag$^{-/-}$ hosts (28). Effector FoxP3$^+$CD49b$^+$ T cells, particularly those coexpressing KLRG1, comprise the majority of the Foxp3$^+$ population in peripheral lymphoid tissues, but not the thymus of β_2m$^{-/-}$A$^b\beta^{-/-}$ mice, suggesting that they develop extrathymically. The presence of cells expressing this same phenotype in normal mice raised the possibility that they also represented an extrathymically derived population. Alternatively, in normal mice, up-regulation of CD49b and KLRG1 may be secondary to progressive differentiation of the effector FoxP3$^+$ T cells. We took advantage of the rapid turnover, presumably in response to ubiquitous Ags, of the effector Foxp3$^+$ T cells in vivo to distinguish between these two possibilities. Mice were treated with an anti-MHC class II Ab to determine whether blocking MHC class II recognition would have a selective effect on the thymic-derived vs the purported thymic-independent subset of CD4$^+$Foxp3$^+$ CD103$^+$ cells. Blockade of MHC class II in both wild-type and MHC class I-deficient mice led to the preferential depletion of the CD49b$^-$ subset with a corresponding enrichment in the CD49$^+$ subset of CD103$^+$FoxP3$^+$ T cells. Although not definitive, this result was consistent with the MHC class I/II independence and extrathymic origin of CD49b$^+$ cells in normal mice. The nature of the ligand driving proliferation of the thymic-independent subset is an important subject for future studies.

The effector FoxP3$^+$ T cell subsets described in the present study share an activated expression pattern with respect to several different surface markers, including CD103. We relied on this marker for identifying and purifying effector cells because of its uniform and distinct expression by effector-phenotype FoxP3$^+$ T cells, particularly those found in the MHC-deficient strains. It is important to note that effector FoxP3$^+$ T cells shared an activated expression pattern with respect to several different surface markers, not only CD103. CD103 does not appear to play a direct role in the suppressor function of FoxP3$^+$ T cells, as CD4$^+$CD25$^+$ T cells from CD103$^{-/-}$ mice are fully capable of preventing colitis in immune-deficient recipients (38). We also find that the CD49b$^+$KLRG1$^+$FoxP3$^+$ subset is present at normal levels in CD103$^{-/-}$ mice, arguing against an obligatory role for CD103 in the development of effector FoxP3$^+$ T cell subsets (data not shown). In contrast, the expression of CD103 on Foxp3$^+$ T regulatory cells may be important in certain situations to mediate the retention of T regulatory cells at certain epithelial sites (39–41) via its interaction with E-cadherin expressed on epithelial cells (42). As CD103 expression can be induced by T cell activation in the presence of TGF-β (43), it is possible that the expression of CD103 by the effector FoxP3$^+$ subset is secondary to their exposure to a TGF-β-rich milieu during their development in the thymus. However, TGF-β1$^{-/-}$ mice contain normal numbers of CD4$^+$CD25$^+$CD103$^+$ thymocytes and peripheral T cell-type mice (44).

Taken together, the results of these studies reveal a remarkable heterogeneity in the Foxp3$^+$ population of T regulatory cells. We have confirmed and extended previous results that have demonstrated that the subpopulation of Foxp3$^+$CD103$^+$ effector T cells represent an effector T cell subset. Moreover, our observations in the K14 mice suggest that the effector cells may be the products of a separate lineage of T regulatory cell development in the thymus rather than a stage in the normal process of T regulatory cell differentiation. A comparison of the TCR repertoire (45, 46) of naive compared with effector Foxp3$^+$ T cells should be of interest as the latter, based on the in vivo activation state, appear to have a higher affinity for self than the naive subpopulation. Lastly, the ability of both the thymic-derived and thymic-independent populations of effector Foxp3$^+$ T cells to suppress T effector function nonspecifically and to home to sites of nonspecific inflammation raises the possibility that their role in immune regulation may be distinct from naive T regulatory cells. If similar populations can be identified in humans, differential manipulations of distinct Foxp3$^+$ T regulatory populations may be of therapeutic importance.

Disclosures

The authors have no financial conflict of interest.

References

1. Shevach, E. M. 2006. From vanilla to 28 flavors: multiple varieties of T regulatory cells. *Immunity* 25: 195–201.
2. Wildin, R. S., F. Ramsdell, J. Peake, F. Faravelli, J. L. Casanova, N. Buist, E. Levy-Lahad, M. Mazzella, O. Goulet, L. Perroni, et al. 2001. X-linked neonatal diabetes mellitus, enteropathy and endocrinopathy syndrome is the human equivalent of mouse scurfy. *Nat. Genet.* 27: 18–20.
3. Bennett, C. L., J. Christie, F. Ramsdell, M. E. Brunkow, P. J. Ferguson, L. Whitesell, T. E. Kelly, F. T. Saulsbury, P. F. Chance, and H. D. Ochs. 2001. The immune dysregulation, polyendocrinopathy, enteropathy, X-linked syndrome (IPEX) is caused by mutations of FOXP3. *Nat. Genet.* 27: 20–21.
4. Fontenot, J. D., M. A. Gavin, and A. Y. Rudensky. 2003. Foxp3 programs the development and function of CD4$^+$CD25$^+$ regulatory T cells. *Nat. Immunol.* 4: 330–336.
5. Hori, S., T. Nomura, and S. Sakaguchi. 2003. Control of regulatory T cell development by the transcription factor Foxp3. *Science* 299: 1057–1061.
6. Khattri, R., T. Cox, S. A. Yasayko, and F. Ramsdell. 2003. An essential role for Scurfin in CD4$^+$CD25$^+$ T regulatory cells. *Nat. Immunol.* 4: 337–342.
7. von Boehmer, H. 2005. Mechanisms of suppression by suppressor T cells. *Nat. Immunol.* 6: 338–344.
8. Thornton, A. M., and E. M. Shevach. 1998. CD4$^+$CD25$^+$ immunoregulatory T cells suppress polyclonal T cell activation in vitro by inhibiting interleukin 2 production. *J. Exp. Med.* 188: 287–296.
9. Itoh, M., T. Takahashi, N. Sakaguchi, Y. Kuniyasu, J. Shimizu, F. Otsuka, and S. Sakaguchi. 1999. Thymus and autoimmunity: production of CD25$^+$CD4$^+$ naturally anergic and suppressive T cells as a key function of the thymus in maintaining immunologic self-tolerance. *J. Immunol.* 162: 5317–5326.
10. McHugh, R. S., M. J. Whitters, C. A. Piccirillo, D. A. Young, E. M. Shevach, M. Collins, and M. C. Byrne. 2002. CD4$^+$CD25$^+$ immunoregulatory T cells: gene expression analysis reveals a functional role for the glucocorticoid-induced TNF receptor. *Immunity* 16: 311–323.
11. Lehmann, J., J. Huehn, M. de la Rosa, F. Maszyna, U. Kretschmer, V. Krenn, M. Brunner, A. Scheffold, and A. Hamann. 2002. Expression of the integrin $\alpha_E\beta_7$ identifies unique subsets of CD25$^+$ as well as CD25$^-$ regulatory T cells. *Proc. Natl. Acad. Sci. USA* 99: 13031–13036.
12. Nakamura, K., A. Kitani, I. Fuss, A. Pedersen, N. Harada, H. Nawata, and W. Strober. 2004. TGF-β1 plays an important role in the mechanism of CD4$^+$CD25$^+$ regulatory T cell activity in both humans and mice. *J. Immunol.* 172: 834–842.
13. Huehn, J., K. Siegmund, J. C. Lehmann, C. Siewert, U. Haubold, M. Feuerer, G. F. Debes, J. Lauber, O. Frey, G. K. Przybylski, U. Niesner, M. de la Rosa, et al. 2004. Developmental stage, phenotype, and migration distinguish naive- and effector/memory-like CD4$^+$ regulatory T cells. *J. Exp. Med.* 199: 303–313.
14. Fisson, S., G. Darrasse-Jeze, E. Litvinova, F. Septier, D. Klatzmann, R. Liblau, and B. L. Salomon. 2003. Continuous activation of autoreactive CD4$^+$CD25$^+$ regulatory T cells in the steady state. *J. Exp. Med.* 198: 737–746.
15. Jordan, M. S., A. Boesteanu, A. J. Reed, A. L. Petrone, A. E. Holenbeck, M. A. Lerman, A. Naji, and A. J. Caton. 2001. Thymic selection of CD4$^+$CD25$^+$ regulatory T cells induced by an agonist self-peptide. *Nat. Immunol.* 2: 301–306.
16. van Santen, H. M., C. Benoist, and D. Mathis. 2004. Number of T reg cells that differentiate does not increase upon encounter of agonist ligand on thymic epithelial cells. *J. Exp. Med.* 200: 1221–1230.
17. Bensinger, S. J., A. Bandeira, M. S. Jordan, A. J. Caton, and T. M. Laufer. 2001. Major histocompatibility complex class II-positive cortical epithelium mediates the selection of CD4$^+$25$^+$ immunoregulatory T cells. *J. Exp. Med.* 194: 427–438.
18. Wan, Y. Y., and R. A. Flavell. 2005. Identifying Foxp3-expressing suppressor T cells with a bicistronic reporter. *Proc. Natl. Acad. Sci. USA* 102: 5126–5131.
19. Fontenot, J. D., J. P. Rasmussen, L. M. Williams, J. L. Dooley, A. G. Farr, and A. Y. Rudensky. 2005. Regulatory T cell lineage specification by the forkhead transcription factor foxp3. *Immunity* 22: 329–341.
20. Bienvenu, B., B. Martin, C. Auffray, C. Cordier, C. Becourt, and B. Lucas. 2005. Peripheral CD8$^+$CD25$^+$ T lymphocytes from MHC class II-deficient mice exhibit regulatory activity. *J. Immunol.* 175: 246–253.
21. Krajina, T., F. Leithauser, and J. Reimann. 2004. MHC class II-independent CD25$^+$CD4$^+$CD8$\alpha\beta^+$ $\alpha\beta$ T cells attenuate CD4$^+$ T cell-induced transfer colitis. *Eur. J. Immunol.* 34: 705–714.
22. Madsen, L., N. Labrecque, J. Engberg, A. Dierich, A. Svejgaard, C. Benoist, D. Mathis, and L. Fugger. 1999. Mice lacking all conventional MHC class II genes. *Proc. Natl. Acad. Sci. USA* 96: 10338–10343.
23. Stephens, G. L., R. S. McHugh, M. J. Whitters, D. A. Young, D. Luxenberg, B. M. Carreno, M. Collins, and E. M. Shevach. 2004. Engagement of glucocorticoid-induced TNFR family-related receptor on effector T cells by its ligand mediates resistance to suppression by CD4$^+$CD25$^+$ T cells. *J. Immunol.* 173: 5008–5020.
24. Herzenberg, L. A., J. Tung, W. A. Moore, L. A. Herzenberg, and D. R. Parks. 2006. Interpreting flow cytometry data: a guide for the perplexed. *Nat. Immunol.* 7: 681–685.

25. Fontenot, J. D., J. L. Dooley, A. G. Farr, and A. Y. Rudensky. 2005. Developmental regulation of Foxp3 expression during ontogeny. *J. Exp. Med.* 202: 901–906.
26. Urdahl, K. B., J. C. Sun, and M. J. Bevan. 2002. Positive selection of MHC class Ib-restricted $CD8^+$ T cells on hematopoietic cells. *Nat. Immunol.* 3: 772–779.
27. Laufer, T. M., J. DeKoning, J. S. Markowitz, D. Lo, and L. H. Glimcher. 1996. Unopposed positive selection and autoreactivity in mice expressing class II MHC only on thymic cortex. *Nature* 383: 81–85.
28. Gonzalez, A., I. Andre-Schmutz, C. Carnaud, D. Mathis, and C. Benoist. 2001. Damage control, rather than unresponsiveness, effected by protective $DX5^+$ T cells in autoimmune diabetes. *Nat. Immunol.* 2: 1117–1125.
29. Pellicci, D. G., K. J. Hammond, J. Coquet, K. Kyparissoudis, A. G. Brooks, K. Kedzierska, R. Keating, S. Turner, S. Berzins, M. J. Smyth, and D. I. Godfrey. 2005. DX5/CD49b-positive T cells are not synonymous with CD1d-dependent NKT cells. *J. Immunol.* 175: 4416–4425.
30. Herman, A. E., G. J. Freeman, D. Mathis, and C. Benoist. 2004. $CD4^+CD25^+$ T regulatory cells dependent on ICOS promote regulation of effector cells in the prediabetic lesion. *J. Exp. Med.* 199: 1479–1489.
31. Chen, Z., A. E. Herman, M. Matos, D. Mathis, and C. Benoist. 2005. Where $CD4^+CD25^+$ T reg cells impinge on autoimmune diabetes. *J. Exp. Med.* 202: 1387–1397.
32. Thornton, A. M., and E. M. Shevach. 2000. Suppressor effector function of $CD4^+CD25^+$ immunoregulatory T cells is antigen nonspecific. *J. Immunol.* 164: 183–190.
33. Takahashi, T., Y. Kuniyasu, M. Toda, N. Sakaguchi, M. Itoh, M. Iwata, J. Shimizu, and S. Sakaguchi. 1998. Immunologic self-tolerance maintained by $CD25^+CD4^+$ naturally anergic and suppressive T cells: induction of autoimmune disease by breaking their anergic/suppressive state. *Int. Immunol.* 10: 1969–1980.
34. Walker, L. S., A. Chodos, M. Eggena, H. Dooms, and A. K. Abbas. 2003. Antigen-dependent proliferation of $CD4^+CD25^+$ regulatory T cells in vivo. *J. Exp. Med.* 198: 249–258.
35. Klein, L., K. Khazaie, and H. von Boehmer. 2003. In vivo dynamics of antigen-specific regulatory T cells not predicted from behavior in vitro. *Proc. Natl. Acad. Sci. USA* 100: 8886–8891.
36. Cozzo, C., J. Larkin III, and A. J. Caton. 2003. Cutting edge: self-peptides drive the peripheral expansion of $CD4^+CD25^+$ regulatory T cells. *J. Immunol.* 171: 5678–5682.
37. Sarnacki, S., B. Begue, H. Buc, F. Le Deist, and N. Cerf-Bensussan. 1992. Enhancement of CD3-induced activation of human intestinal intraepithelial lymphocytes by stimulation of the β_7-containing integrin defined by HML-1 monoclonal antibody. *Eur. J. Immunol.* 22: 2887–2892.
38. Annacker, O., J. L. Coombes, V. Malmstrom, H. H. Uhlig, T. Bourne, B. Johansson-Lindbom, W. W. Agace, C. M. Parker, and F. Powrie. 2005. Essential role for CD103 in the T cell-mediated regulation of experimental colitis. *J. Exp. Med.* 202: 1051–1061.
39. Cepek, K. L., C. M. Parker, J. L. Madara, and M. B. Brenner. 1993. Integrin $\alpha_E\beta_7$ mediates adhesion of T lymphocytes to epithelial cells. *J. Immunol.* 150: 3459–3470.
40. Schon, M. P., A. Arya, E. A. Murphy, C. M. Adams, U. G. Strauch, W. W. Agace, J. Marsal, J. P. Donohue, H. Her, D. R. Beier, et al. 1999. Mucosal T lymphocyte numbers are selectively reduced in integrin α_E (CD103)-deficient mice. *J. Immunol.* 162: 6641–6649.
41. Suffia, I., S. K. Reckling, G. Salay, and Y. Belkaid. 2005. A role for CD103 in the retention of $CD4^+CD25^+$ Treg and control of *Leishmania major* infection. *J. Immunol.* 174: 5444–5455.
42. Cepek, K. L., S. K. Shaw, C. M. Parker, G. J. Russell, J. S. Morrow, D. L. Rimm, and M. B. Brenner. 1994. Adhesion between epithelial cells and T lymphocytes mediated by E-cadherin and the $\alpha_E\beta_7$ integrin. *Nature* 372: 190–193.
43. Parker, C. M., K. L. Cepek, G. J. Russell, S. K. Shaw, D. N. Posnett, R. Schwarting, and M. B. Brenner. 1992. A family of β_7 integrins on human mucosal lymphocytes. *Proc. Natl. Acad. Sci. USA* 89: 1924–1928.
44. Mamura, M., W. Lee, T. J. Sullivan, A. Felici, A. L. Sowers, J. P. Allison, and J. J. Letterio. 2004. CD28 disruption exacerbates inflammation in Tgf-$\beta1^{-/-}$ mice: in vivo suppression by $CD4^+CD25^+$ regulatory T cells independent of autocrine TGF-β1. *Blood* 103: 4594–4601.
45. Hsieh, C. S., Y. Zheng, Y. Liang, J. D. Fontenot, and A. Y. Rudensky. 2006. An intersection between the self-reactive regulatory and nonregulatory T cell receptor repertoires. *Nat. Immunol.* 7: 401–410.
46. Pacholczyk, R., H. Ignatowicz, P. Kraj, and L. Ignatowicz. 2006. Origin and T cell receptor diversity of $Foxp3^+CD4^+CD25^+$ T cells. *Immunity* 25: 249–259.